Epigenetic regulation of Matrix metalloproteinase-1 and -3 expression in *Mycobacterium tuberculosis* Infection

Authors: Rachel C. Moores[1¶], Sara Brilha[1,2¶], Frans Schutgens[1], Paul T Elkington[1,3], Jon S. Friedland[1*]

Affiliations:

1- Section of Infectious Diseases and Immunity, Imperial College London, UK

2- Centre for Inflammation and Tissue Repair, Respiratory Medicine, University College London, UK

3- National Institute of Health Research (NIHR) Respiratory Biomedical Research Unit, Faculty of Medicine, University of Southampton, Southampton, UK

[¶]Joint first authors; contributed equally to this work.

*** Correspondence:**

Jon S. Friedland

E-mail: j.friedland@imperial.ac.uk

Abstract

In pulmonary tuberculosis (TB), the inflammatory immune response against *Mycobacterium tuberculosis* (Mtb) is associated with tissue destruction and cavitation, which drives disease transmission, chronic lung disease and mortality. Matrix metalloproteinase (MMP)-1 is a host enzyme critical for the development of cavitation. MMP expression has been shown to be epigenetically regulated in other inflammatory diseases, but the importance of such mechanisms in Mtb-associated induction of MMP-1 is unknown. We investigated the role of changes in histone acetylation in Mtb-induced MMP expression using inhibitors of histone deacetylases (HDACs) and histone acetyltransferases (HAT), HDAC siRNA, promoter-reporter constructs and chromatin immunoprecipitation assays.

Mtb-infection decreased Class I HDAC gene expression by over 50% in primary human monocyte-derived macrophages but not in normal human bronchial epithelial cells (NHBEs). Non-selective inhibition of HDAC activity decreased MMP-1/-3 expression by Mtb-stimulated macrophages and NHBEs, while class I HDAC inhibition increased MMP-1 secretion by Mtb-stimulated NHBEs. MMP-3 expression, but not MMP-1, was downregulated by siRNA silencing of HDAC1. Inhibition of HAT activity also significantly decreased MMP-1/-3 secretion by Mtb-infected macrophages. The MMP-1 promoter region between -2001 and -2942 base pairs from the transcriptional start site was key in control of Mtb-driven MMP-1 gene expression. Histone H3 and H4 acetylation and RNA Pol II binding in the MMP-1 promoter region were increased in stimulated NHBEs.

In summary, epigenetic modification of histone acetylation via HDAC and HAT activity has a key regulatory role in Mtb-dependent gene expression and secretion of MMP-1 and -3, enzymes which drive human immunopathology. Manipulation of epigenetic regulatory mechanisms may have potential as a host-directed therapy to improve outcomes in the era of rising TB drug resistance.

Keywords: *Mycobacterium tuberculosis;* matrix metalloproteinases; histone deacetylases; histone acetyltransferases; epigenetics

1. Introduction

Tuberculosis (TB) remains a major global health problem, with 10.4 million new cases and 1.8 million deaths per year (WHO 2016). The rapid emergence of widespread drug resistance necessitates new strategies to improve the efficacy of treatment in TB, both to decrease transmission and to improve patient outcomes. Ideally, such therapies will shorten the duration of therapy, which is currently a minimum of 6 months and may be years in drug-resistant disease. Host-directed therapies are increasingly of interest in TB (Wallis and Hafner 2015).

The primary site of *Mycobacterium tuberculosis* (Mtb) infection is the lung and pulmonary disease is characterized by granulomatous inflammation with destruction of lung parenchyma. The outcome of infection is very variable between hosts, and the factors determining this are not well understood, although host genetics and innate immune responses are important determinants of disease (Thuong, Dunstan et al. 2008, Azad, Sadee et al. 2012). Matrix metalloproteinases (MMPs) are zinc-dependent endopeptidases which have key roles in tissue repair and in diseases characterized by inflammatory tissue destruction such as emphysema (McGarry Houghton 2015). MMPs are key mediators of inflammatory cell migration, and modulators of chemokine and cytokine signaling (Dobaczewski, Gonzalez-Quesada et al. 2010, Ong, Elkington et al. 2014). MMP activity is strongly implicated in the immunopathogenesis of TB. Our group and others demonstrated the involvement of MMP-1, the major human collagenase, and its activator MMP-3 (stromelysin-1) in driving pathology in pulmonary TB (Green, Elkington et al. 2010, Elkington, Shiomi et al. 2011, Al Shammari, Shiomi et al. 2015). MMPs are secreted by Mtb-infected monocytes and macrophages, and also by uninfected stromal cells stimulated via intercellular networks (Singh, Saraiva et al. 2014). Epigenetic mechanisms are emerging as major regulators of

MMP activity in non-infectious diseases (Chernov and Strongin 2011, Loffek, Schilling et al. 2011), including chronic lung diseases such as asthma and COPD (Mortaz, Masjedi et al. 2011), but their role in MMP expression in TB is less established.

Epigenetic regulation encompasses all chromosomal modifications that alter gene expression without altering the nucleotide sequence of coding DNA (Bird 2007, Goldberg, Allis et al. 2007). Eukaryotic DNA is packaged as chromatin around octamers of histone proteins, which contain globular domains and negatively charged tails. These are subject to extensive post-translational modification, including acetylation of highly conserved lysine residues. Acetylation of histones H3 and H4, carried out by Histone acetyltransferases (HATs), is associated with increased gene transcription (Bannister and Kouzarides 2011). Conversely, acetyl groups are removed by the histone deacetylases (HDACs), which are divided into four classes. The Class I HDACs (1, 2, 3 and 8) are ubiquitously expressed whereas Class II HDACs (such as HDAC 4 and 5) are selectively expressed in different tissues. HDAC activity is usually associated with silencing of gene expression (de Ruijter, van Gennip et al. 2003, Shahbazian and Grunstein 2007). However, this is not uniformly the case and opposite regulation may occur. For example, HDAC inhibition reduced MMP-9 gene expression in cancer cell lines resulting in a less invasive phenotype (Lee, Choi et al. 2010).

The epigenetic mechanisms regulating inflammatory immune responses in TB is an emerging field. Altered miRNA expression in serum and sputum from TB patients compared to controls has been shown, and potential biomarkers for diagnosis have been identified (Kleinsteuber, Heesch et al. 2013). A growing body of evidence exists to support the importance of epigenetic mechanisms in other respiratory infections, for example altered DNA methylation patterns in asthma patients versus healthy controls have been implicated in the pathogenesis of rhinovirus infection (McErlean, Favoreto et al. 2014). Similarly, altered

DNA (cytosine-5-)-methyltransferase-1 (DMT-1) expression in nasal epithelial cells from smokers was identified as a possible mechanism of increased susceptibility to influenza (Jaspers, Horvath et al. 2010). *In vitro* studies of airway epithelial cells demonstrated increased HDAC2 expression and decreased histone acetylation in respiratory syncytial virus (RSV)-infected cells, while chemical HDAC inhibition restricted RSV replication(Feng, Su et al. 2016). In the current study, we have investigated whether epigenetic modifications, specifically histone acetylation/deacetylation, regulated the characteristic TB-associated expression of MMP-1 and MMP-3 by monocyte-derived macrophages and normal human bronchial epithelial cells (NHBEs), thereby augmenting TB immunopathology. The role of histone acetylation in induction of MMP-1/-3 expression was specifically investigated, since this dynamic epigenetic mark is associated with transcriptional activation. We demonstrate that Mtb infection alters macrophage Class I HDAC expression and that MMP-1 expression induced by Mtb is sensitive to HDAC/HAT inhibition. In addition, increased histone acetylation was seen at MMP-1 and -3 promoter regions compared with unstimulated cells, specifically in the region -2001 to -2942bp of the MMP-1 promoter, which contains key inducible sites activated in Mtb-stimulated cells.

2. Materials & Methods

2.1. Reagents and antibodies

Trichostatin A (TSA) was purchased from Sigma-Aldrich (Gillingham, UK), CBHA, HAT inhibitor II and Anacardic acid (AA) from Calbiochem (Millipore, Watford, UK) and MS-275 from Enzo Life Sciences (Exeter, UK). Primary rabbit anti-human acetyl-histone H3 and acetyl-histone H4 (Millipore) were used for chromatin immunoprecipitation. Primary mouse anti-human HDAC4 and anti-HDAC7 were used for western blot and HRP-linked goat anti-rabbit IgG and goat anti-mouse (all from Cell Signalling, Hertfordshire, UK) were used as secondary antibodies. All other reagents were purchased from Sigma-Aldrich unless otherwise stated.

2.2. *Mycobacterium tuberculosis* culture

Mtb strain H37Rv was cultured from frozen stocks stored at -80°C in Middlebrook 7H9 broth (BD Biosciences, Oxford, UK) supplemented with 10% OADC enrichment medium (BD Biosciences), 0.2% glycerol and 0.02% Tween 20 with agitation at 37°C. Growth was monitored by measuring optical density (OD) using a Biowave cell density meter (WPA, Cambridge, UK). Infection experiments were performed using cultures at mid-log growth (at OD 0.55-0.65) corresponding to 1-2 $x10^8$ CFU/ml. Correlation with optical density was checked by performing colony counts in triplicate on Middlebrook 7H11 agar. Cells were infected at a multiplicity of infection (MOI) of 1 unless otherwise stated.

2.3. Cell culture

Monocytes were adhesion-purified from leukocyte residues from healthy blood donors (NHS Blood Transfusion Service) and differentiated into macrophages for 4 days in RPMI 1640 (Life Technologies, Paisley, UK) supplemented with 10% FBS and 100ng/ml M-CSF (R&D

Systems, Abingdon, UK). After a further 24 hours without M-CSF, the medium was changed for M-SFM (Life Technologies) and cells were infected with *Mycobacterium tuberculosis* H37Rv strain. Cells were pre-treated with chemical inhibitors for 2 hours prior to infection where relevant.

Primary normal human bronchial epithelial cells (NHBEs) (Lonza, Wokingham, UK) were cultured according to the supplier's instructions in supplemented bronchial epithelial growth medium (BEGM). Medium was replaced every 3 days. Cells were sub-cultured at 80% confluence and used at passage 4 or 5.

The alveolar carcinoma cell line A549 (ATCC, Middlesex, UK) was cultured in RPMI 1640 supplemented with 2mM glutamine, 10µg/ml ampicillin and 10% Fetal Bovine Serum (FBS). For experiments cells were seeded at 4x 10^4 cells/cm^2 and stimulated 24 hours later.

2.4. Conditioned medium from Mycobacterium tuberculosis-infected monocytes (CoMTb)

Peripheral blood monocytes isolated as above from healthy blood donors were infected with H37Rv at a multiplicity of infection (MOI) of 1 in RPMI without FBS for 24 hours. The culture medium was then collected and sterilized by passage through a 0.2 µM Anopore syringe filter (Whatman, Brentford, UK). Paired samples of conditioned medium from uninfected monocytes (CoMCont) from the same donor were used as controls.

2.5. MMP ELISAs

Supernatants were collected at 72h post-stimulus, sterile filtered, and MMPs were quantified using the Duoset MMP-1 and MMP-3 ELISA kits (R&D Systems) according to

manufacturer's instructions. Lower limits of sensitivity for the Duoset kits are: 156pg/ml for MMP-1 and 31.2pg/ml for MMP-3. Samples were run with appropriate controls and at dilutions calculated to give readings within the linear range of detection as indicated by the manufacturer.

2.6. Luminex multiplex immunoassay

Quantification of MMP-1, -3, -7 and -9 concentrations was performed using the Fluorokine MultiAnalyte Profiling MMP Base Kit (R&D Systems) and the Luminex platform Bio-Plex 200 (Bio-Rad, Hemel Hempstead, UK) dual laser analyzer. Standard curves were generated using Bio-Plex Manager version 5.0. Lower limits of sensitivity for the Fluorokine Luminex were: 1.1pg/ml for MMP-1, 7.3pg/ml for MMP-3, 6.6pg/ml for MMP-7 and 13.7pg/ml for MMP-9. All samples were run with appropriate controls and were within the linear range of detection as indicated by the manufacturer.

2.7. Transient transfection with promoter-reporter constructs

MMP-1 promoter constructs expressed in the pGL3 firefly (*Photinus pyralis*) luciferase expression vector (Promega, Southampton, UK) were a gift of Professor Ian Clark (University of East Anglia, Norwich, UK). The full-length wild-type MMP-1 promoter construct (WT) comprised a 4372 bp sequence upstream of the MMP-1 transcriptional start site. Deletion constructs ranged in size from 3830bp to 517bp (Wang, Guan et al. 2014). MMP-3 promoter constructs were designed in-house and cloned into the pGL3 vector. Truncations were generated using primers that incorporated restriction enzyme sites within the sequence of interest: MMP3-1R 5'-GCTTTACTTAGATCTATGTTGTCTC-3'; MMP3-4F 5'-GCTAGAGCTAGCAAGGATCCTGCAC-3'; MMP3-6R 5'-CTTCATTTCCACAAGCTTTACTTAGCTCT-3'; MMP3-7F 5'-

GTTTTCCTCCTCGAGAACCAGCAAATCC-3'; MMP3-8F 5'-CATCATTCTACTGAGCTCTTACTCCCAAG-3'; MMP3-9F 5'-CCATGTCTGTAATCCTAGCACTTTGAG-3'; MMP3-10F 5'-GTTCAGTGTGGAAAATAGAGTAGCAGAGG-3'; MMP3-11 – F 5'-GATGGATTCTCGAGTTCAACTTCAAAGCATCTG-3'; MMP3-12 – R 5'-GAGACAGAGATCTCACTATGTTGCCC-3'. PCR products of the 3kb MMP-3 promoter region were digested in one step using NheI and BglII, followed by BamHI and BglII for cloning into pGL4 and pBSK vectors. Shorter fragments of the original 3kb MMP-3 promoter region were digested using HindIII and XhoI for MMP3-7F/MMP3-6R; SacI and HindIII for MMP3-8F/MMP3-6R and MMP3-9F/MMP3-6R, and KpnI and HindIII for MMP3-10F/MMP3-6R. After 2h incubation at 37^{o}C, enzymes were inactivated at 68^{o}C for 20min. The constructs generated were 2183bp, 1612bp and 642bp in length. WT MMP-1/-3 promoters and respective truncations were inserted upstream of the luciferase reporter gene in the pGL3 vector. The PRL-TK plasmid constitutively expressing *Renilla* luciferase was used to control for transfection efficiency.

A549 cells were transfected when 60% confluent with FuGene 6 (Roche, Lewes, UK), and 0.8μg plasmid DNA or control plasmid DNA. 16 hours after transfection the cells were stimulated according to the experimental conditions. 24 hours later cells were washed once in PBS and lysed in passive lysis buffer (Promega). Luciferase assays were performed using the Promega Dual-Luciferase Reporter Assay kit (Promega) using an L-Max 2 luminometer (Molecular Devices, Sunnydale, CA, USA).

2.8. Real-time PCR

After 24 hours incubation in the specified experimental settings, cells were lysed in TRI-reagent and total RNA extracted with the PureLink RNA mini kit (Life Technologies) with on-column DNase treatment. RNA concentrations and purity were evaluated using a Nanodrop spectrophotometer (Thermo Scientific, Wilmington, DE, USA). 1µg of sample RNA was reverse transcribed using the Quantitect RT Kit (Qiagen, Crawley, UK) according to the manufacturer's instructions. Real-time PCR was performed using Brilliant II qPCR mastermix (Agilent, UK) on a Stratagene Mx3000p platform (Stratagene, La Jolla, USA). The thermal profile was 10min at 95°C, followed by 40 to 45 cycles of 30 sec at 95°C and 1min at 60°C. The cycle threshold (Ct) at which amplification entered the exponential phase was determined for each well and analyte. 18S ribosomal RNA, β-actin and GAPDH RNA were used as reference genes. The following primers and probes were used to analyze target and reference genes:

MMP-1 forward primer 5'- AAGATGAAAGGTGGACCAACAATT -3'; reverse primer 5' - CCAAGAGAATGGCCGAGTTC -3' and probe 5'-FAM CAGAGAGTACAACTTACATC GTGTTGCGGCTC-TAMRA-3'; GAPDH (forward primer 5'-CGCTTCGCTCTCTGCTCC T-3'; reverse primer 5'- CGACCAAATCCGTTGACTCC-3' and probe 5'-HEX-CGTCGCC AGCCGAGCCACAT -TAMRA-3'(both from Sigma-Aldrich); MMP-3 Hs00968305_m1; HDAC1 Hs02621185_s1; HDAC2 Hs00231032_m1; HDAC3 Hs0018730_m1; HDAC4 Hs01041638_m1; HDAC5 Hs00608366_m1; HDAC8 Hs00218503_m1 ; 18S 4308329 and β-actin 431088E (all Taqman primer and probe mixes from Life Technologies). Cts from target genes were normalized to Cts for the reference genes which were measured simultaneously for each PCR assay performed.

2.9. Transfection of epithelial cells with siRNA

ON-TARGETplus SMARTpool siRNA oligonucleotides and transfection reagents were purchased from Dharmacon (Thermo Scientific). NHBEs were cultured in complete medium and transfected at 60-70% confluence. siRNA and Lipofectamine 2000 were diluted in Optimem and used at final concentrations of 30nM and 25µg/ml respectively. After 4 hours each well was washed with PBS and fresh BEGM was added. The cells were then rested overnight prior to stimulation with the experimental conditions. For analysis of mRNA expression, cells were lysed and total RNA was extracted 24 hours after stimulation. For analysis of protein expression cell culture supernatants were collected for ELISA and cells were washed in PBS and lysed in Western lysis buffer 48 hours post-stimulation.

2.10. Chromatin Immunoprecipitation assay (ChIP)

Magna-ChIP kits and antibodies were purchased from Millipore (Watford, UK) and used according to manufacturer's instructions. The rabbit polyclonal anti-acetyl-Histone H4 antibody was raised against tetra acetylated H4 and recognizes intermediately acetylated H4, but not acetylation on lysine 16. The rabbit polyclonal anti-acetyl-Histone 3 antibody was raised against acetylated N-terminus of H3.

Cells were cultured in 100mm or 150mm tissue culture dishes until confluent then stimulated as previously described. Cells were fixed with fresh 1% paraformaldehyde solution for 10min and the reaction was stopped with glycine. Chromatin was sheared by sonication with a Covaris S2 ultra-sonicator using an Adaptive Focused Acoustics intensifier (KBioscience). Settings were as follows: temperature 6-8°C, duty cycle 20%, intensity 8, 200 cycles/burst, 15 cycles of 30sec, 2 x 10^7 cell equivalents/ml. Immunoprecipitation was performed overnight at 4°C with 1x10^6 cell equivalents per condition. Purified DNA was eluted and PCR performed using SYBR Green JumpStart Taq Readymix. Reactions were performed in

triplicate on the Stratagene Mx3000P platform (Stratagene, La Jolla, USA). The following custom unlabeled primers were designed in-house and supplied by Sigma. MMP-1 transcription start site forward primer 5'-TGGGATATTGGAGCAGCAAG-3'and reverse primer 5'-AGCTGTGCATACTGGCCTTT -3' (product size 82bp); -500bp MMP-1 promoter forward primer 5'-TAAGGGAAGCCAT GGTGCTA-3'; reverse primer 5'-AGGTTCCCTTCTGCCTTTGT-3' (product size 65bp); -2kbp MMP-1 promoter forward primer 5'TTGCCAGATGGGACAGTGTA-3' and reverse 5'-TCAGGAAAGCAGCATGTGAC-3' (product size 123 bp); -4kbp MMP-1 promoter forward primer 5'-CTTGAGGCCAGGAGTTTGAG-3' and reverse primer 5'-ACCACCAT GTCCCACTGATT-3' (product size 89bp).

These assays were not performed in technical triplicates due to the number of cells required per condition.

2.11. Statistics

Unless otherwise stated, results shown are from experiments performed in triplicate and representative of at least two independent experiments. Comparisons between two groups were made using the Student t-test (two-tailed with significance set as $p<0.05$). For comparison of three or more groups, one-way ANOVA was used with Tukey's correction for multiple comparisons. Unless otherwise stated in figure legends, graphs show mean values for triplicate samples and error bars are the standard deviation (s.d.).

3. Results

3.1. Class I HDACs are suppressed by Mtb infection of macrophages

Experiments were designed to investigate epigenetic regulation of TB immunopathology, first investigating whether Mtb infection of macrophages altered Class I HDAC expression. Expression of Class I HDACs was repressed by Mtb-infection, with a 68% decrease in HDAC1, 69% in HDAC2, 76% in HDAC3 and 58% in HDAC8 compared with uninfected controls (all $p<0.05$) (Fig. 1A-1D). Next, we examined monocyte network-dependent stimulation of NHBEs by CoMTb. In contrast to macrophage stimulation by Mtb, CoMTb-stimulation of NHBEs did not significantly alter accumulation of any class I HDAC mRNAs (Fig. 1E-1H). Expression of Class II HDACs 4 and 5 was also examined by RT-PCR. HDAC4 mRNA accumulation was increased by 48% in Mtb-infected macrophages, while no difference was observed for HDAC5 (Fig. 1I, 1J). Increase in HDAC4 protein level was confirmed by western blot (Fig. S1). Class II HDAC expression in CoMTb-stimulated NHBEs was similar to control conditions (Fig. 1K, 1L). Thus, exposure to live Mtb selectively suppressed macrophage class I HDAC expression.

3.2. Non-selective HDAC inhibition reduces MMP-1 and -3 expression in macrophages and NHBEs during Mtb infection.

Next, we investigated whether histone acetylation status affected MMP expression using the non-selective HDAC inhibitor (HDACi) Trichostatin A (TSA). 100ng/ml TSA markedly decreased Mtb-stimulated MMP-1 and MMP-3 secretion by macrophages (Fig. 2A, B). In NHBEs, TSA significantly decreased baseline MMP-1 secretion by over 50% ($p<0.05$; Fig 2C). CoMTb-stimulated MMP-1 secretion was decreased by TSA treatment although this did not reach statistical significance (Fig. 2C). In contrast, CoMTb-stimulated MMP-3 secretion

was significantly reduced in a dose-dependent manner by 25% with 1ng/ml TSA (from 2.4ng/ml to 1.8ng/ml) and by 72% with 10ng/ml TSA (685pg/ml) (Fig. 2D).

Further experiments were performed using an alternative chemical HDAC inhibitor, CBHA (m-Carboxycinnamic Acid bis-Hydroxamide), to confirm that the observed effects were due to HDAC inhibition and not non-specific. Pre-treatment of macrophages with 4μM CBHA before Mtb infection decreased MMP-1 secretion by 77% (from 8.89ng/ml to 2.05ng/ml) and MMP-3 secretion to undetectable levels (Fig. 2E, F). CoMTb-driven MMP-1 secretion was reduced by CBHA treatment in a dose-dependent manner. 5μM CBHA reduced MMP-1 secretion by 41% (from 797 to 473 pg/ml; $p<0.05$; Fig. 2G), while 1μM CBHA was sufficient to completely inhibit CoMTb-induced MMP-3 secretion ($p<0.0001$; Fig. 2H). These results indicate that HDACs may differ between cell types, each with specific MMP regulatory pathways.

The HDAC class I- selective inhibitor MS-275 (1μM) inhibited Mtb-driven macrophage MMP-1 secretion by 92% and reduced MMP-3 concentrations by 94.4% (Fig. 2I, J). This supports the earlier finding, and implies a key regulatory role for class I HDACs in macrophages MMP-1/-3 expression. In contrast, MS-275 enhanced MMP-1 secretion by both unstimulated ($p<0.05$) and CoMTb-stimulated NHBEs ($p<0.0001$; Fig. 2K). MS-275 at a low concentration of 1μM increased MMP-3 secretion 4.6-fold compared to CoMTb alone ($p<0.05$), but this was not observed at the higher concentration of 10μM MS-275 (Fig. 2L), possibly due to sub-lethal cell toxicity which could not be detected by cell viability experiments. The effects of these HDAC inhibitors on MMP secretion were selective, since neither TSA nor 1μM MS-275 significantly altered MMP -7 secretion by Mtb infected macrophages (Fig. 2M, 2N).

3.3. Silencing HDAC1 expression does not affect CoMTb-driven MMP-1 expression

Next, we investigated whether a specific class I HDAC enzyme was necessary for CoMTb-induced MMP-1 and -3 expression. HDAC1 mRNA was reduced by more than 80% in CoMTb-stimulated cells transfected with 30nM HDAC1 siRNA compared to non-targeting (NT) siRNA or untransfected controls (Fig. 3A; $p=0.001$). Despite efficient HDAC1 silencing, no significant differences were observed in MMP-1 mRNA accumulation (Fig. 3B). Consistent with this, MMP-1 concentrations were 3204 pg/ml in CoMTb/HDAC1 siRNA treated samples compared to 3746 pg/ml in the CoMTb/NT siRNA samples (Fig. 3C). MMP-3 mRNA was upregulated 3-fold by CoMTb stimulation but no difference was observed between NT and HDAC1 siRNA transfected NHBEs (Fig. 3D). MMP-3 protein secretion in the NT-transfected cells was upregulated by CoMTb ($p<0.001$), and MMP-3 secretion was reduced by 30% in HDAC1 siRNA-transfected cells compared to NT-transfected conditions ($p<0.01$; Fig 3E). Silencing of HDAC2 in epithelial cells with siRNA was also effective and increased CoMTb-stimulated MMP-1, but not MMP-3, mRNA expression compared to CoMTb alone ($p<0.05$; Fig. 3G, 3H). Silencing HDAC3 with siRNA did not affect MMP-1 or MMP-3 expression (Fig. S2A-C).

3.4. Macrophage-derived MMP-1 and -3 gene expression and secretion during Mtb-infection are blocked by HAT inhibition.

Next, the role of HAT activity was investigated using the inhibitor HATi II. 10μM HATi II significantly decreased MMP-1 secretion from Mtb-infected macrophages by 56% (from 5029pg/ml to 2187pg/ml) and mRNA accumulation by 62% (Fig. 4A, B). MMP-3 secretion was decreased from 1653pg/ml to 190pg/ml ($p<0.0001$, Fig. 4C). There was a non-significant

trend to decreased MMP-3 mRNA accumulation with HATi II treatment (Fig. 4D). HATi II treatment did not affect MMP-7 secretion in response to Mtb infection (Fig. S3).

A second HAT inhibitor, anacardic acid (AA, 10 μM), reduced Mtb-infected macrophage MMP-1 secretion by 74% (from 5029pg/ml to 1302pg/ml; $p<0.0001$) (Fig 4E). Similarly, a significant decrease in MMP-1 secretion was also detected in stimulated NHBE cells pre-treated with AA (Fig. S4). Secretion of MMP-3 in Mtb-infected macrophages was also inhibited by 10μM AA ($p<0.01$; Fig.4F). The AA compound is closely related to salicylic acid, and has been reported to have some antimicrobial activity, including against Mtb (Swamy, Suma et al. 2007, Omanakuttan, Nambiar et al. 2012). We therefore investigated whether these results might be secondary to an effect on Mtb growth, but this was not altered in broth cultures containing AA at concentrations between 2 to 25μM (Fig. 4G). These experiments support the hypothesis that HAT activity is required for inducible expression of MMP-1 and MMP-3 in macrophages and NHBEs stimulated with Mtb.

3.5. MMP-1 and MMP-3 promoter-reporter analysis in TB

Plasmid promoter-reporter constructs of the MMP-1 and MMP-3 promoter regions were transfected into A549 respiratory epithelial cells to investigate the effect of Mtb-stimulation on promoter activity. A schematic representation of the relevant region of the human MMP-1 promoter region is shown in figure 5A. CoMTb treatment increased promoter activity of the WT (wild-type) construct by more than 3-fold compared to controls ($p=0.02$; Fig 5B). CoMTb-mediated promoter activation was significantly enhanced by 98% and 71% in the 3830bp and 2942bp constructs respectively compared to CoMtb-stimulated WT ($p<0.01$). Further truncation of the promoter resulted in loss of CoMTb-driven promoter activity. The MMP-3 promoter, examined using similar methodology, showed a progressive reduction in

both basal and CoMTb-stimulated promoter activity with truncation of the construct from 1612bp to 642bp in length (Fig. 5C) compared to WT. The 1612bp truncation is missing a stromelysin platelet-derived growth factor responsive element (SPRE; -1659 to -1643bp) and part of the stromelysin IL-1 responsive element (SIRE; -1614 to -1595bp), and in addition, the 642bp truncation is missing 4 AP-1, 2 STAT3 and 1 c-rel binding sites.

3.6. CoMTb-driven MMP-1 expression and increased histone acetylation in the promoter region

To further investigate whether epigenetic modifications of the MMP-1 promoter controlled the response to CoMTb, we examined the histone acetylation status of the MMP-1 promoter region by chromatin immunoprecipitation. Preliminary experiments using the respiratory epithelial A549 cell line suggested marked increases in histone H4 acetylation with CoMTb treatment at 1 and 2 hour post-stimulus (data not shown). In primary NHBEs, RNA Polymerase II binding to the MMP-1 promoter was increased between 10 to 15-fold in cells after 2h of CoMTb treatment (Fig. 6A). Histone H3 acetylation was increased 2 hours post-stimulation, and was approximately 3-fold greater than under control conditions in the proximal promoter, and 5-fold higher than control when measured 2 kbp upstream of the MMP-1 transcriptional start site (Fig. 6B). Detection of acetylated histone H4 after 2 hours of CoMTb-stimulation was also increased across the MMP-1 promoter region. Histone H4 acetylation was 10-fold higher at -2kbp and -500bp, and 6-fold higher than unstimulated controls at the transcriptional start site (Fig. 6C).

4. Discussion

Upregulation of MMP-1 in TB is a critical event for the development of cavitation (Elkington, Shiomi et al. 2011). Previous studies from our group and other have demonstrated that Mtb-stimulation upregulates MMP-1 expression, which is enzymatically active and able to degrade type I collagen, the main component of the lung's ECM (Al Shammari, Shiomi et al. 2015, Brilha, Sathyamoorthy et al. 2017, Tezera, Bielecka et al. 2017). Expression of other MMPs is also induced in pulmonary TB (Kubler, Luna et al. 2015, Brilha, Sathyamoorthy et al. 2017), and MMPs are implicated in central nervous system immunopathology (Majeed, Singh et al. 2016, Ong, Pabisiak et al. 2017). In this study we demonstrated that expression of MMP-1 and -3 in response to Mtb is controlled by epigenetic changes in histone acetylation. HDACs are canonically considered to be negative regulators of gene expression, and we showed a change in the profile of HDAC expression following Mtb-infection of macrophages. Downregulation of Class I HDAC gene expression was observed with a concomitant and selective upregulation of HDAC4 but not HDAC5. In contrast, in respiratory epithelial cells, Class I and Class II HDAC expression were unchanged after CoMtb-stimulation, implying that this is a cell-type specific effect. TLR signaling is known to induce changes in HDAC expression and activity (Aung, Schroder et al. 2006), and our findings are consistent with published evidence of selective changes in macrophage HDAC expression in response to specific inflammatory stimuli (Bell, Winkler et al. 2012). Our data show that Mtb-infection of macrophages induces a change in the cellular HDAC profile. We went on to investigate the likely effects of this change by performing experiments in which MMP responses were examined under conditions of both general and specific HDAC blockade.

Non-selective HDAC inhibition using TSA and the bipolar hybrid CBHA suppressed Mtb-driven MMP-1 and -3 secretion and mRNA accumulation in primary epithelial cells and

macrophages. Such a paradoxical effect on MMP expression has been previously reported in an *in vitro* model of arthritis, where chondrocyte collagenase activity was inhibited by TSA (Wang, Song et al. 2009). In an mouse model of arthritis, TSA also inhibited MMP-1, -3 and -13 expression (Nasu, Nishida et al. 2008). Similarly, LPS-induced MMP expression by murine bone marrow-derived macrophages was inhibited by TSA (Roger, Lugrin et al. 2010). The Class I selective HDAC inhibitor MS-275 had contrasting effects: increasing basal and CoMTb-stimulated MMP-1 and -3 secretion in epithelial cells, while in Mtb-infected macrophages, it decreased MMP-1/-3 secretion. Similar inhibition of cytokine-induced MMP-1 was seen in MS-275 treated human chondrocytes (Culley, Hui et al. 2013). The effects of MS-275 may be due to selective inhibition of HDAC1 at lower concentrations, and additional effects on the activity of HDAC2 and 3 at higher concentrations (Khan, Jeffers et al. 2008). Individual HDAC enzymes are likely to play different roles in regulation of MMP expression, and since these chemicals affect function of multiple HDACs, it is impossible to dissect the relative contribution of each HDAC by a chemical inhibition approach alone.

The increased secretion of MMP-1 and -3 from NHBEs observed with Class I HDAC inhibition, as compared to non-selective HDAC inhibition, is consistent with the premise that Class I HDACs are key negative regulators of MMP expression. HDAC1 was shown to be recruited to the MMP-9 promoter site, reducing histone H3 acetylation and NF-κB recruitment, leading to repression of MMP-9 expression in fibrosarcoma cells(Mittelstadt and Patel 2012).

The enhancement of CoMTb-stimulated MMP expression observed with MS-275 led us to hypothesize that silencing the expression of HDAC1 might similarly increase inducible MMP expression. The catalytic activity of HDAC 1 and 2 is reliant on their incorporation as

heterodimers into multi-protein assemblies (Alland, David et al. 2002) and therefore we expected that silencing either HDAC 1 or HDAC 2 would affect MMP expression. However, in spite of a high efficiency of HDAC1-silencing, MMP-1 expression was unaffected, and MMP-3 secretion was decreased in HDAC1-silenced cells. In contrast, upregulation of MMP-1 in CoMTb-stimulated conditions was further enhanced with HDAC2 inhibition, suggesting that MS-275 could be having its effect via inhibition of HDAC2 rather than HDAC1. The differing results for HDAC1 and HDAC2 silencing are unexpected given the close homology between these proteins, and consequently further dissection of their relative contributions to control of MMP expression is needed. In other experimental systems, different HDACs have been implicated in MMP regulation and there may be cell and stimulus specificity in host responses. In synovial fibroblasts from arthritis patients, HDAC1 siRNA enhanced TNFα-induced MMP-1 expression(Horiuchi, Morinobu et al. 2009), whereas HDAC4 was identified as a negative regulator of MMP-1 expression(Maciejewska-Rodrigues, Karouzakis et al. 2009).

Consistent with the hypothesis that epigenetic modifications regulate MMP secretion in TB, expression of MMP-1 and -3 were both suppressed by HAT inhibition with HATi II. Experiments using a structurally unrelated HAT inhibitor, anacardic acid, generated consistent data. Similarly, in human dermal fibroblasts exposed to UV-light, anacardic acid inhibited MMP-1 expression, as did siRNA-silencing of p300 expression. Increased HAT activity and histone H3 acetylation and decreased HDAC activity preceded changes in MMP-1 gene expression (Kim, Lipke et al. 2010). The finding that both HAT and HDAC inhibition decreased MMP-1 and -3 expression, while apparently contradictory, may reflect the complex interdependence of these processes. It is well-recognized that many non-histone substrates of these enzymes exist (Wolffe 1996, Choudhary, Kumar et al. 2009) and indeed

phylogenetic studies have indicated that bacterial HDAC homologues pre-date the existence of histones (Gregoretti, Lee et al. 2004). Lysine acetylation of many non-histone proteins has been shown to be enhanced by HDAC inhibition, for example with MS-275 (Choudhary, Kumar et al. 2009).

Many transcription factors contain such lysine acetylation sites, including cAMP response element binding protein (CREB), whose activity is increased in the presence of TSA(Michael, Asahara et al. 2000). CREB can be acetylated at three sites, enhancing its transcription factor activity, and HDAC8 is known to act on the CREB acetylation sites (Lu, Hutchins et al. 2003). The NF-κB family of transcription factors is also subject to post-translational modification including acetylation as well as phosphorylation(Chen, Mu et al. 2002). Myocyte enhancer factor-2 (MEF2) is deacetylated by HDAC3, which also acts on the HATs PCAF and p300/CBP(Gregoire, Xiao et al. 2007). In addition to transcription factors and HATs, the HDACs themselves contain lysine acetylation sites, as do a number of structural and regulatory proteins (Moser, Hagelkruys et al. 2014). Therefore, it is difficult to dissect out the relative contribution of inhibition of histone acetylation/deacetylation compared to effects on these other substrates when considering the effects of chemical inhibitors, and our findings indicate a complex interplay of signaling pathways occurs during infection.

The promoter-reporter analysis showed that inhibitory elements located 4372 to 2942bp upstream from the MMP-1 transcriptional start site decrease promoter activation, since deletion of this region enhanced CoMTb-driven promoter activity. The area between -2942 and -2001bp contains several critical elements required for the induction of gene expression, including a putative NF-κB binding site. There is also an AP-1 site at -1950bp just proximal

to the -2001bp truncation that might be functionally disrupted by this truncation. There is substantial evidence that MMP-1 expression is regulated by both NF-κB and AP-1 family transcription factors (Barchowsky, Frleta et al. 2000, Kumar, Ray et al. 2009, Green, Elkington et al. 2010), and our data support a central role. Similarly, multiple transcription binding sites may be important in MMP-3 promoter function. Our chromatin immunoprecipitation studies demonstrated that CoMTb stimulation leads to increased H3 and H4 acetylation at the MMP-1 promoter region. Histone acetylation was an early event after CoMTb stimulation occurring concurrently with binding of RNA Pol II to the MMP-1 promoter.

In summary, MMP-1 and 3 expression in TB is regulated by HDAC and HAT activity. MMP-1 upregulation, as a result of epigenetic control, has the potential to drive tissue damage in the lung, thereby facilitating spread of infection and development of pathology. Chemical inhibition suggests that HDAC and HAT activity is necessary for inducible expression of MMP-1 and -3 in Mtb-infected macrophages, but that different mechanisms operate in NHBEs, where class I HDACs appear to act as a brake on collagenase expression. This is a selective effect, as MMP-7, which is constitutively expressed in MDMs and upregulated by Mtb infection, was unaffected by HDAC and HAT inhibition.
The minimal inhibition of MMP responses seen with siRNA targeting individual class I HDACs implies there may be some redundancy of function. Increased histone acetylation in the MMP-1 promoter region follows Mtb stimulation, favoring RNA Pol II binding, and results in upregulation of MMP gene transcription and enzyme secretion. Tissue breakdown mediated by MMP activity is a key event in TB immunopathology and manipulation of host

epigenetic changes have potential applications as host directed therapy in the era of rising drug resistance in TB.

Conflict of Interest Statement: The authors declare no conflict of interest.

Authors' contributions: JSF conceived the project. RM, PTE, and JSF designed the experiments and analyzed the data. RM, SB, and FS, performed the experiments and generated the data. SB, RM, PTE, and JSF wrote the manuscript which was reviewed and final version approved by all authors.

Funding: RCM was a Wellcome Trust Clinical Research Fellow. SB was supported by the Portuguese Foundation for Science and Technology (FCT). SB and JSF were supported by the Rosetrees Trust and Breathing Matters charities. JSF acknowledges support of the Biomedical Research Centre at Imperial College.

References

Al Shammari, B., T. Shiomi, L. Tezera, M. K. Bielecka, V. Workman, T. Sathyamoorthy, F. Mauri, S. N. Jayasinghe, B. D. Robertson, J. D'Armiento, J. S. Friedland and P. T. Elkington (2015). The Extracellular Matrix Regulates Granuloma Necrosis in Tuberculosis. *J Infect Dis* **212**(3):463-73.

Alland, L., G. David, H. Shen-Li, J. Potes, R. Muhle, H. C. Lee, H. Hou, Jr., K. Chen and R. A. DePinho (2002). Identification of mammalian Sds3 as an integral component of the Sin3/histone deacetylase corepressor complex.*Mol Cell Biol* **22**(8): 2743-2750.

Aung, H. T., K. Schroder, S. R. Himes, K. Brion, W. van Zuylen, A. Trieu, H. Suzuki, Y. Hayashizaki, D. A. Hume, M. J. Sweet and T. Ravasi (2006). LPS regulates proinflammatory gene expression in macrophages by altering histone deacetylase expression. *FASEB J* **20**(9): 1315-1327.

Azad, A. K., W. Sadee and L. S. Schlesinger (2012). Innate immune gene polymorphisms in tuberculosis. *Infect Immun* **80**(10): 3343-3359.

Bannister, A. J. and T. Kouzarides (2011). Regulation of chromatin by histone modifications. *Cell Res* **21**(3): 381-395.

Barchowsky, A., D. Frleta and M. P. Vincenti (2000). Integration of the NF-kappaB and mitogen-activated protein kinase/AP-1 pathways at the collagenase-1 promoter: divergence of IL-1 and TNF-dependent signal transduction in rabbit primary synovial fibroblasts. *Cytokine* **12**(10): 1469-1479.

Bell, R. D., E. A. Winkler, I. Singh, A. P. Sagare, R. Deane, Z. Wu, D. M. Holtzman, C. Betsholtz, A. Armulik, J. Sallstrom, B. C. Berk and B. V. Zlokovic (2012). Apolipoprotein E controls cerebrovascular integrity via cyclophilin A. *Nature* **485**(7399): 512-516.

Bird, A. (2007). Perceptions of epigenetics. *Nature* **447**(7143): 396-398.

584 Brilha, S., T. Sathyamoorthy, L. H. Stuttaford, N. F. Walker, R. J. Wilkinson, S. Singh, R. C.
585 Moores, P. T. Elkington and J. S. Friedland (2017). Early Secretory Antigenic Target-6
586 Drives Matrix Metalloproteinase-10 Gene Expression and Secretion in Tuberculosis. *Am J*
587 *Respir Cell Mol Biol* **56**(2): 223-232.
588 Chen, L. F., Y. Mu and W. C. Greene (2002). Acetylation of RelA at discrete sites regulates
589 distinct nuclear functions of NF-kappaB. *EMBO J* **21**(23): 6539-6548.
590 Chernov, A. V. and A. Y. Strongin (2011). Epigenetic regulation of matrix
591 metalloproteinases and their collagen substrates in cancer. *Biomol Concepts* **2**(3): 135-147.
592 Choudhary, C., C. Kumar, F. Gnad, M. L. Nielsen, M. Rehman, T. C. Walther, J. V. Olsen
593 and M. Mann (2009). Lysine acetylation targets protein complexes and co-regulates major
594 cellular functions. *Science* **325**(5942): 834-840.
595 Culley, K. L., W. Hui, M. J. Barter, R. K. Davidson, T. E. Swingler, A. P. Destrument, J. L.
596 Scott, S. T. Donell, S. Fenwick, A. D. Rowan, D. A. Young and I. M. Clark (2013). Class I
597 histone deacetylase inhibition modulates metalloproteinase expression and blocks cytokine-
598 induced cartilage degradation. *Arthritis Rheum* **65**(7): 1822-1830.
599 de Ruijter, A. J., A. H. van Gennip, H. N. Caron, S. Kemp and A. B. van Kuilenburg (2003).
600 Histone deacetylases (HDACs): characterization of the classical HDAC family. *Biochem J*
601 **370**(Pt 3): 737-749.
602 Dobaczewski, M., C. Gonzalez-Quesada and N. G. Frangogiannis (2010). The extracellular
603 matrix as a modulator of the inflammatory and reparative response following myocardial
604 infarction. *J Mol Cell Cardiol* **48**(3): 504-511.
605 Elkington, P., T. Shiomi, R. Breen, R. K. Nuttall, C. A. Ugarte-Gil, N. F. Walker, L. Saraiva,
606 B. Pedersen, F. Mauri, M. Lipman, D. R. Edwards, B. D. Robertson, J. D'Armiento and J. S.
607 Friedland (2011). MMP-1 drives immunopathology in human tuberculosis and transgenic
608 mice. *J Clin Invest* **121**(5): 1827-1833.

609 Feng, Q., Z. Su, S. Song, H. Chiu, B. Zhang, L. Yi, M. Tian and H. Wang (2016). Histone
610 deacetylase inhibitors suppress RSV infection and alleviate virus-induced airway
611 inflammation. *Int J Mol Med* **38**(3): 812-822.
612 Goldberg, A. D., C. D. Allis and E. Bernstein (2007). Epigenetics: a landscape takes shape.
613 *Cell* **128**(4): 635-638.
614 Green, J. A., P. T. Elkington, C. J. Pennington, F. Roncaroli, S. Dholakia, R. C. Moores, A.
615 Bullen, J. C. Porter, D. Agranoff, D. R. Edwards and J. S. Friedland (2010). *Mycobacterium*
616 *tuberculosis* upregulates microglial matrix metalloproteinase-1 and -3 expression and
617 secretion via NF-kappaB- and Activator Protein-1-dependent monocyte networks. *J Immunol*
618 **184**(11): 6492-6503.
619 Gregoire, S., L. Xiao, J. Nie, X. Zhang, M. Xu, J. Li, J. Wong, E. Seto and X. J. Yang (2007).
620 Histone deacetylase 3 interacts with and deacetylates myocyte enhancer factor 2. *Mol Cell*
621 *Biol* **27**(4): 1280-1295.
622 Gregoretti, I. V., Y. M. Lee and H. V. Goodson (2004). Molecular evolution of the histone
623 deacetylase family: functional implications of phylogenetic analysis. *J Mol Biol* **338**(1): 17-
624 31.
625 Horiuchi, M., A. Morinobu, T. Chin, Y. Sakai, M. Kurosaka and S. Kumagai (2009).
626 Expression and function of histone deacetylases in rheumatoid arthritis synovial fibroblasts. *J*
627 *Rheumatol* **36**(8): 1580-1589.
628 Jaspers, I., K. M. Horvath, W. Zhang, L. E. Brighton, J. L. Carson and T. L. Noah (2010).
629 Reduced expression of IRF7 in nasal epithelial cells from smokers after infection with
630 influenza. *Am J Respir Cell Mol Biol* **43**(3): 368-375.
631 Khan, N., M. Jeffers, S. Kumar, C. Hackett, F. Boldog, N. Khramtsov, X. Qian, E. Mills, S.
632 C. Berghs, N. Carey, P. W. Finn, L. S. Collins, A. Tumber, J. W. Ritchie, P. B. Jensen, H. S.

633 Lichenstein and M. Sehested (2008). Determination of the class and isoform selectivity of
634 small-molecule histone deacetylase inhibitors. *Biochem J* **409**(2): 581-589.
635 Kim, D. H., E. A. Lipke, P. Kim, R. Cheong, S. Thompson, M. Delannoy, K. Y. Suh, L. Tung
636 and A. Levchenko (2010). Nanoscale cues regulate the structure and function of macroscopic
637 cardiac tissue constructs. *Proc Natl Acad Sci U S A* **107**(2): 565-570.
638 Kleinsteuber, K., K. Heesch, S. Schattling, M. Kohns, C. Sander-Julch, G. Walzl, A.
639 Hesseling, E. Mayatepek, B. Fleischer, F. M. Marx and M. Jacobsen (2013). Decreased
640 expression of miR-21, miR-26a, miR-29a, and miR-142-3p in CD4(+) T cells and peripheral
641 blood from tuberculosis patients. *PLoS One* **8**(4): e61609.
642 Kubler, A., B. Luna, C. Larsson, N. C. Ammerman, B. B. Andrade, M. Orandle, K. W. Bock,
643 Z. Xu, U. Bagci, D. J. Molura, J. Marshall, J. Burns, K. Winglee, B. A. Ahidjo, L. S. Cheung,
644 M. Klunk, S. K. Jain, N. P. Kumar, S. Babu, A. Sher, J. S. Friedland, P. T. Elkington and W.
645 R. Bishai (2015). *Mycobacterium tuberculosis* dysregulates MMP/TIMP balance to drive
646 rapid cavitation and unrestrained bacterial proliferation. *J Pathol* **235**(3): 431-444.
647 Kumar, D., A. Ray and B. K. Ray (2009). Transcriptional synergy mediated by SAF-1 and
648 AP-1: critical role of N-terminal polyalanine and two zinc finger domains of SAF-1. *J Biol*
649 *Chem* **284**(3): 1853-1862.
650 Lee, K. H., E. Y. Choi, M. K. Kim, K. O. Kim, B. I. Jang, S. W. Kim, S. W. Kim, S. K. Song
651 and J. R. Kim (2010). Inhibition of histone deacetylase activity down-regulates urokinase
652 plasminogen activator and matrix metalloproteinase-9 expression in gastric cancer. *Mol Cell*
653 *Biochem* **343**(1-2): 163-171.
654 Loffek, S., O. Schilling and C. W. Franzke (2011). Series "matrix metalloproteinases in lung
655 health and disease": Biological role of matrix metalloproteinases: a critical balance. *Eur*
656 *Respir J* **38**(1): 191-208.

Lu, Q., A. E. Hutchins, C. M. Doyle, J. R. Lundblad and R. P. Kwok (2003). Acetylation of cAMP-responsive element-binding protein (CREB) by CREB-binding protein enhances CREB-dependent transcription. *J Biol Chem* **278**(18): 15727-15734.

Maciejewska-Rodrigues, H., E. Karouzakis, S. Strietholt, H. Hemmatazad, M. Neidhart, C. Ospelt, R. E. Gay, B. A. Michel, T. Pap, S. Gay and A. Jüngel (2009). Epigenetics and rheumatoid arthritis: The role of SENP1 in the regulation of MMP-1 expression. *Journal of Autoimmunity* **35**(1): 15-22.

Majeed, S., P. Singh, N. Sharma and S. Sharma (2016). Role of matrix metalloproteinase -9 in progression of tuberculous meningitis: a pilot study in patients at different stages of the disease. *BMC Infect Dis* **16**(1): 722.

McErlean, P., S. Favoreto, Jr., F. F. Costa, J. Shen, J. Quraishi, A. Biyasheva, J. J. Cooper, D. M. Scholtens, E. F. Vanin, M. F. de Bonaldo, H. Xie, M. B. Soares and P. C. Avila (2014). Human rhinovirus infection causes different DNA methylation changes in nasal epithelial cells from healthy and asthmatic subjects. *BMC Med Genomics* **7**: 37.

McGarry Houghton, A. (2015). Matrix metalloproteinases in destructive lung disease. *Matrix Biol* **44-46C**: 167-174.

Michael, L. F., H. Asahara, A. I. Shulman, W. L. Kraus and M. Montminy (2000). The phosphorylation status of a cyclic AMP-responsive activator is modulated via a chromatin-dependent mechanism. *Mol Cell Biol* **20**(5): 1596-1603.

Mittelstadt, M. L. and R. C. Patel (2012). AP-1 mediated transcriptional repression of matrix metalloproteinase-9 by recruitment of histone deacetylase 1 in response to interferon beta. *PLoS One* **7**(8): e42152.

Mortaz, E., M. R. Masjedi, P. J. Barnes and I. M. Adcock (2011). Epigenetics and chromatin remodeling play a role in lung disease. *Tanaffos* **10**(4): 7-16.

Moser, M. A., A. Hagelkruys and C. Seiser (2014). Transcription and beyond: the role of mammalian class I lysine deacetylases. *Chromosoma* **123**(1-2): 67-78.

Nasu, Y., K. Nishida, S. Miyazawa, T. Komiyama, Y. Kadota, N. Abe, A. Yoshida, S. Hirohata, A. Ohtsuka and T. Ozaki (2008). Trichostatin A, a histone deacetylase inhibitor, suppresses synovial inflammation and subsequent cartilage destruction in a collagen antibody-induced arthritis mouse model. *Osteoarthritis and Cartilage* **16**(6): 723-732.

Omanakuttan, A., J. Nambiar, R. M. Harris, C. Bose, N. Pandurangan, R. K. Varghese, G. B. Kumar, J. A. Tainer, A. Banerji, J. J. Perry and B. G. Nair (2012). Anacardic acid inhibits the catalytic activity of matrix metalloproteinase-2 and matrix metalloproteinase-9. *Mol Pharmacol* **82**(4): 614-622.

Ong, C. W., P. T. Elkington and J. S. Friedland (2014). Tuberculosis, pulmonary cavitation, and matrix metalloproteinases. *Am J Respir Crit Care Med* **190**(1): 9-18.

Ong, C. W., P. J. Pabisiak, S. Brilha, P. Singh, F. Roncaroli, P. T. Elkington and J. S. Friedland (2017). Complex regulation of neutrophil-derived MMP-9 secretion in central nervous system tuberculosis. *J Neuroinflammation* **14**(1): 31.

Roger, T., J. Lugrin, D. Le Roy, G. Goy, M. Mombelli, T. Koessler, X. C. Ding, A. L. Chanson, M. K. Reymond, I. Miconnet, J. Schrenzel, P. Francois and T. Calandra (2010). Histone deacetylase inhibitors impair innate immune responses to Toll-like receptor agonists and to infection. *Blood* **117**(4): 1205-1217.

Shahbazian, M. D. and M. Grunstein (2007). Functions of site-specific histone acetylation and deacetylation. *Annu Rev Biochem* **76**: 75-100.

Singh, S., L. Saraiva, P. T. Elkington and J. S. Friedland (2014). Regulation of matrix metalloproteinase-1, -3, and -9 in *Mycobacterium tuberculosis*-dependent respiratory networks by the rapamycin-sensitive PI3K/p70(S6K) cascade. *FASEB J* **28**(1): 85-93.

Swamy, B. N., T. K. Suma, G. V. Rao and G. C. Reddy (2007). Synthesis of isonicotinoylhydrazones from anacardic acid and their in vitro activity against *Mycobacterium smegmatis*. *Eur J Med Chem* **42**(3): 420-424.

Tezera, L. B., M. K. Bielecka, A. Chancellor, M. T. Reichmann, B. A. Shammari, P. Brace, A. Batty, A. Tocheva, S. Jogai, B. G. Marshall, M. Tebruegge, S. N. Jayasinghe, S. Mansour and P. T. Elkington (2017). Dissection of the host-pathogen interaction in human tuberculosis using a bioengineered 3-dimensional model. *Elife* **6**. pii: e21283.

Thuong, N. T., S. J. Dunstan, T. T. Chau, V. Thorsson, C. P. Simmons, N. T. Quyen, G. E. Thwaites, N. Thi Ngoc Lan, M. Hibberd, Y. Y. Teo, M. Seielstad, A. Aderem, J. J. Farrar and T. R. Hawn (2008). Identification of tuberculosis susceptibility genes with human macrophage gene expression profiles. *PLoS Pathog* **4**(12): e1000229.

Wallis, R. S. and R. Hafner (2015). Advancing host-directed therapy for tuberculosis. *Nat Rev Immunol* **15**(4): 255-263.

Wang, P., P. P. Guan, T. Wang, X. Yu, J. J. Guo, K. Konstantopoulos and Z. Y. Wang (2014). Interleukin-1beta and cyclic AMP mediate the invasion of sheared chondrosarcoma cells via a matrix metalloproteinase-1-dependent mechanism. *Biochim Biophys Acta* **1843**(5): 923-933.

Wang, X., Y. Song, J. L. Jacobi and R. S. Tuan (2009). Inhibition of histone deacetylases antagonized FGF2 and IL-1beta effects on MMP expression in human articular chondrocytes. *Growth Factors* **27**(1): 40-49.

WHO (2016). Global Tuberculosis Report 2016.

Wolffe, A. P. (1996). Histone deacetylase: a regulator of transcription. *Science* **272**(5260): 371-372.

730 **Figure legends**

731 **Figure 1- Class I HDAC expression is downregulated in Mtb-infected macrophages.**
732 Macrophages were infected with H37Rv at an MOI of 1, while NHBEs were stimulated with
733 CoMTb (1:5 dilution), for 24h before total RNA was extracted for Class I HDAC gene
734 expression analysis. Figures show mRNA levels (AU) for: (A, E) HDAC1, (B, F) HDAC2,
735 (C, G) HDAC3, (D, H) HDAC8 for macrophages and NHBEs respectively. For Class II
736 HDAC analysis, RNA was processed in a similar manner and figures show an (I, K) HDAC4
737 mRNA and (J, L) HDAC5 mRNA accumulation for macrophages and NHBEs. Bars
738 represent mean ± s.d. and analysis was performed using Student t-test. *$p<0.05$; **$p<0.01$.
739 AU- Arbitrary units.
740

741 **Figure 2- Mtb-driven MMP-1 and -3 secretion is suppressed by HDAC inhibition.**
742 Macrophages and NHBEs were pre-incubated with 1-100ng/ml TSA (A-D), 0.1-5µM CBHA
743 (E-H) or 1-10µM MS-275 (I-L) to inhibit HDAC activity, prior to infection with H37Rv
744 (MOI 1) or stimulation with CoMTb (1:5 dilution) for 72h, then MMP-1 and -3 secretion was
745 measured. Pre-treatment with TSA supressed: (A) MMP-1 and (B) MMP-3 secretion from
746 Mtb-infected macrophages. In CoMTb stimulated NHBEs (C), MMP-1 secretion was
747 unaltered and (D) MMP-3 secretion decreased with TSA treatment. Pre-treatment with
748 CBHA supressed: (E) MMP-1 and (F) MMP-3 secretion from Mtb-infected macrophages and
749 (G) MMP-1 and (H) MMP-3 secretion from CoMTb-stimulated NHBEs. The Class I
750 selective HDAC inhibitor MS-275 supressed: (I) MMP-1 and (J) MMP-3 secretion from Mtb-
751 infected macrophages, while it increased (K) MMP-1 secretion and decreased (L) MMP-3
752 secretion from CoMtb-stimulated NHBEs. Secretion of MMP-7 was not affected by (M) TSA
753 and (N) 1µM MS-275 treatment in Mtb-infected macrophages. Bars represent mean ± s.d.

and analysis was performed using one-way ANOVA with Tukey's post-test. *p<0.05; **p<0.01; ****p<0.0001. CBHA- m-Carboxycinnamic Acid bis-Hydroxamide.

Figure 3- Silencing of HDAC1 and HDAC2 expression does not inhibit CoMTb-driven MMP-1 gene expression.

NHBEs were transfected with 30nM non-targeting (NT), HDAC1 or HDAC2 specific siRNA, or treated with transfection reagent alone. Cells were then stimulated with CoMTb (1:5) for 24h or 48h. (A) HDAC1 mRNA normalized to the reference gene ACTB shows siRNA suppresses mRNA levels. (B) MMP-1 mRNA accumulation and (C) MMP-1 secretion following HDAC1 silencing are not significantly suppressed by siRNA. (D) MMP-3 mRNA accumulation remained unchanged, while (E) MMP-3 secretion decreased following HDAC1 silencing. (F) HDAC2 mRNA normalised to the reference gene ACTB and accumulation was silenced by HDAC2 siRNA. HDAC2 silencing increased MMP-1 mRNA accumulation (G) and did not affect MMP-3 mRNA accumulation (H) in CoMtb stimulated NHBEs. mRNA of target genes was normalized to mRNA of the reference gene ACTB. Bars represent mean ± s.d. and analysis was performed using one-way ANOVA with Tukey's post-test.*p<0.05; **p<0.01; ****p<0.0001; ns- non significant. ACTB- beta-actin; HDAC- histone deacetylase siRNA; NT- non target siRNA.

Figure 4- HATi II inhibits Mtb-driven MMP-1 and -3 secretion.

Macrophages were pre-incubated with 10µM HATi II or 1-10µM AA prior to infection with H37Rv (MOI 1). Total RNA was extracted after 24h and cell culture supernatants were collected after 72h. Pre-treatment with the HATi II supressed : (A) MMP-1 secretion and (B) MMP-1 mRNA accumulation, as well as (C) MMP-3 secretion and (D) MMP-3 mRNA accumulation. Pre-treatment with 1-10µM AA supressed: (E) MMP-1 and (F) MMP-3

secreted concentrations in Mtb-infected macrophages. (G) H37Rv was cultured in the presence of AA 2-25µM and bacterial growth was accessed by OD measurements. Bars represent mean ± s.d. and analysis was performed using one-way ANOVA with Tukey's post-test.*p<0.05; **p<0.01; ****p<0.0001; ns- non significant. ACTB- beta-actin; AA= anacardic acid.

Figure 5- Regulation of MMP-1 and -3 transcription in CoMTb stimulated respiratory epithelial cells.

WT and truncations of the MMP-1 and MMP-3 promoters expressed in the pGL3 firefly luciferase expression vectors were transfected into A549 cells. MMP-1 and -3 promoter activity for each truncation was assessed by relative luciferase activity compared to WT controls. (A) Schematic representation of WT MMP-1 promoter and truncations and relevant transcription factors binding sites. (B) MMP-1 promoter activity is significantly repressed in truncations upstream -2001bp of the transcriptional start site. (C) MMP-3 promoter activity is supressed by truncations upstream -1612bp from the transcriptional start site. Bars represent mean ± s.d. and analysis was performed using one-way ANOVA with Tukey's post-test. *p<0.05; **p<0.01; ***p<0.001. AU- arbitrary unit; WT- wild-type.

Figure 6- Mtb-driven MMP-1 expression is associated with increased RNA Pol II binding and increased histone H3 and H4 acetylation of the MMP-1 promoter.

ChIP assays were performed on NHBEs treated with CoMTb (black triangles) or control medium (grey circles) for 1h (dashed line) or 2h (solid line) post-stimulation. (A) RNA Pol II, (B) acetylated histone H3 and (C) acetylated histone H4 association with the MMP-1 promoter increases after 2h CoMtb stimulation, particularly between -2000bp to -1000bp from the transcriptional start site. Data presented as percentage of the total chromatin input

(% input) and figures are representative of 3 independent experiments. Acetyl H3- acetylated histone H3; Acetyl H4- acetylated histone H4; ChIP- chromatin immunoprecipitation; RNA Pol II- RNA polymerase II.

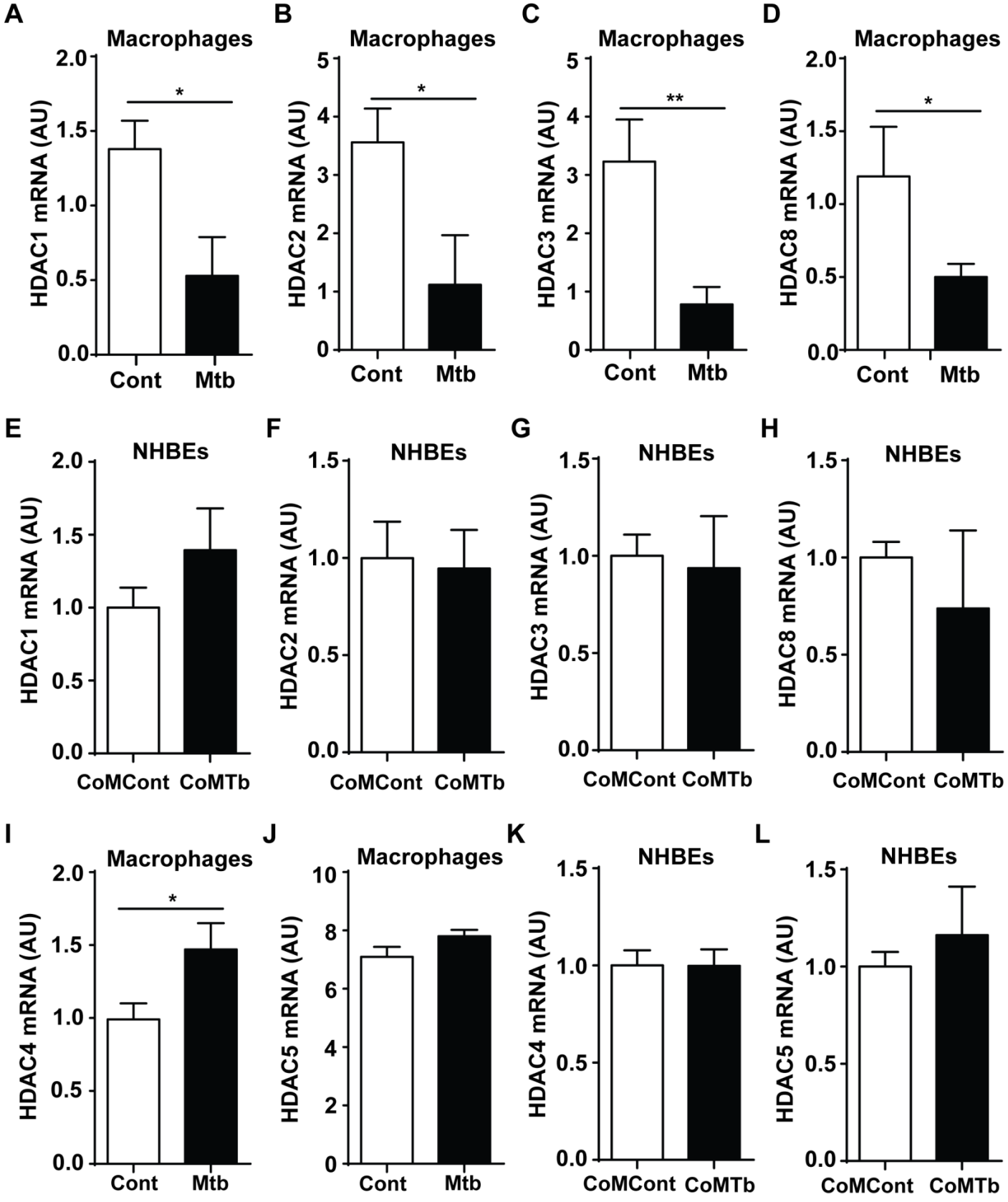
A
Macrophages
HDAC1 mRNA (AU)
2.0
1.5
1.0
0.5
0.0
*
Cont
Mtb
B
Macrophages
HDAC2 mRNA (AU)
5
4
3
2
1
0
*
Cont
Mtb
C
Macrophages
HDAC3 mRNA (AU)
5
4
3
2
1
0
**
Cont
Mtb
D
Macrophages
HDAC8 mRNA (AU)
2.0
1.5
1.0
0.5
0.0
*
Cont
Mtb
E
NHBEs
HDAC1 mRNA (AU)
2.0
1.5
1.0
0.5
0.0
CoMCont
CoMTb
F
NHBEs
HDAC2 mRNA (AU)
1.5
1.0
0.5
0.0
CoMCont
CoMTb
G
NHBEs
HDAC3 mRNA (AU)
1.5
1.0
0.5
0.0
CoMCont
CoMTb
H
NHBEs
HDAC8 mRNA (AU)
1.5
1.0
0.5
0.0
CoMCont
CoMTb
I
Macrophages
HDAC4 mRNA (AU)
2.0
1.5
1.0
0.5
0.0
*
Cont
Mtb
J
Macrophages
HDAC5 mRNA (AU)
10
8
6
4
2
0
Cont
Mtb
K
NHBEs
HDAC4 mRNA (AU)
1.5
1.0
0.5
0.0
CoMCont
CoMTb
L
NHBEs
HDAC5 mRNA (AU)
1.5
1.0
0.5
0.0
CoMCont
CoMTb

Fig. 1

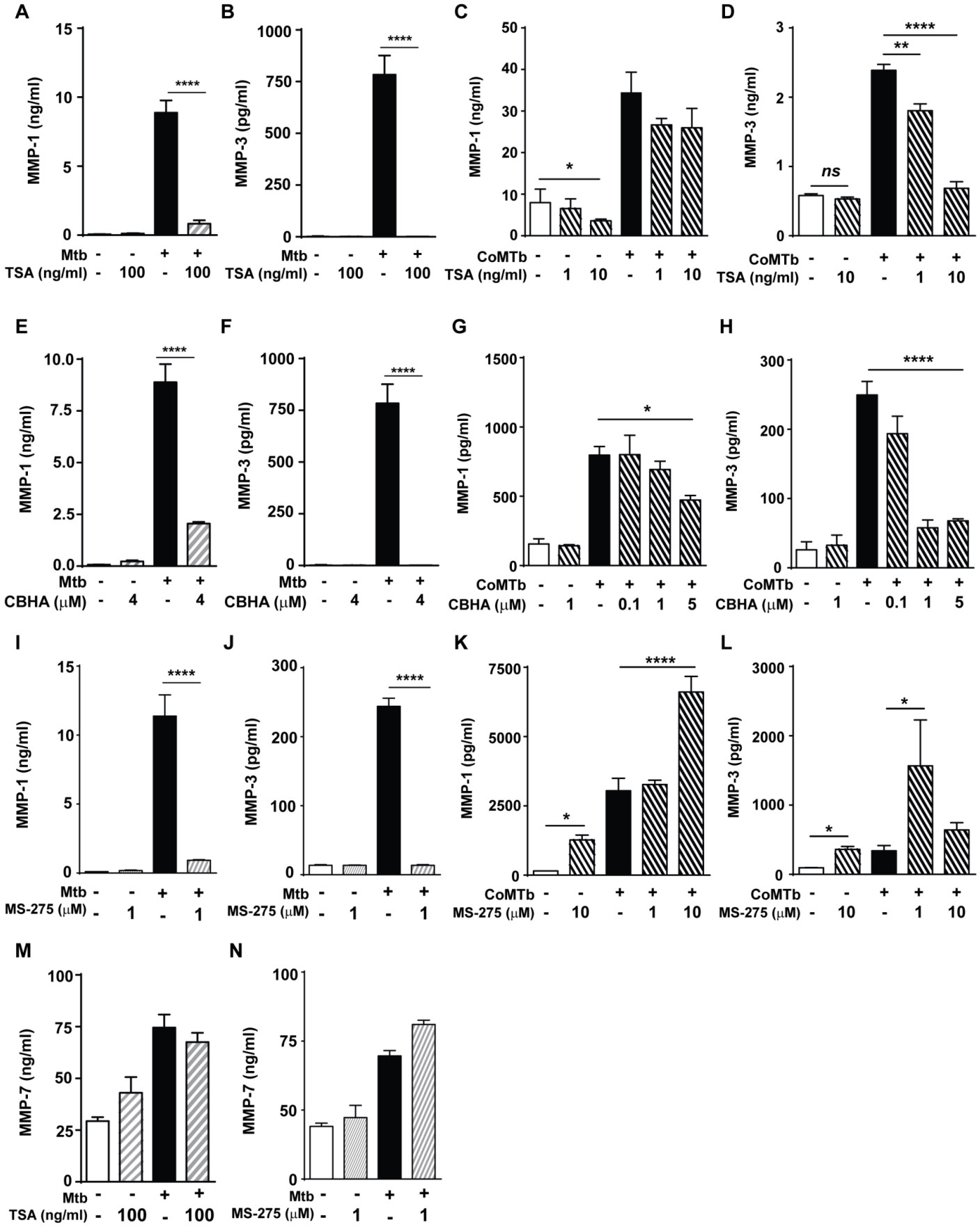
A
MMP-1 (ng/ml)
Mtb - - + +
TSA (ng/ml) - 100 - 100
B
MMP-3 (pg/ml)
Mtb - - + +
TSA (ng/ml) - 100 - 100
C
MMP-1 (ng/ml)
CoMTb - - - + + +
TSA (ng/ml) - 1 10 - 1 10
D
MMP-3 (ng/ml)
ns
CoMTb - - + + +
TSA (ng/ml) - 10 - 1 10
E
MMP-1 (ng/ml)
Mtb - - + +
CBHA (μM) - 4 - 4
F
MMP-3 (pg/ml)
Mtb - - + +
CBHA (μM) - 4 - 4
G
MMP-1 (pg/ml)
CoMTb - - + + + +
CBHA (μM) - 1 - 0.1 1 5
H
MMP-3 (pg/ml)
CoMTb - - + + + +
CBHA (μM) - 1 - 0.1 1 5
I
MMP-1 (ng/ml)
Mtb - - + +
MS-275 (μM) - 1 - 1
J
MMP-3 (pg/ml)
Mtb - - + +
MS-275 (μM) - 1 - 1
K
MMP-1 (pg/ml)
CoMTb - - + + +
MS-275 (μM) - 10 - 1 10
L
MMP-3 (pg/ml)
CoMTb - - + + +
MS-275 (μM) - 10 - 1 10
M
MMP-7 (ng/ml)
Mtb - - + +
TSA (ng/ml) - 100 - 100
N
MMP-7 (ng/ml)
Mtb - - + +
MS-275 (μM) - 1 - 1

Fig. 2

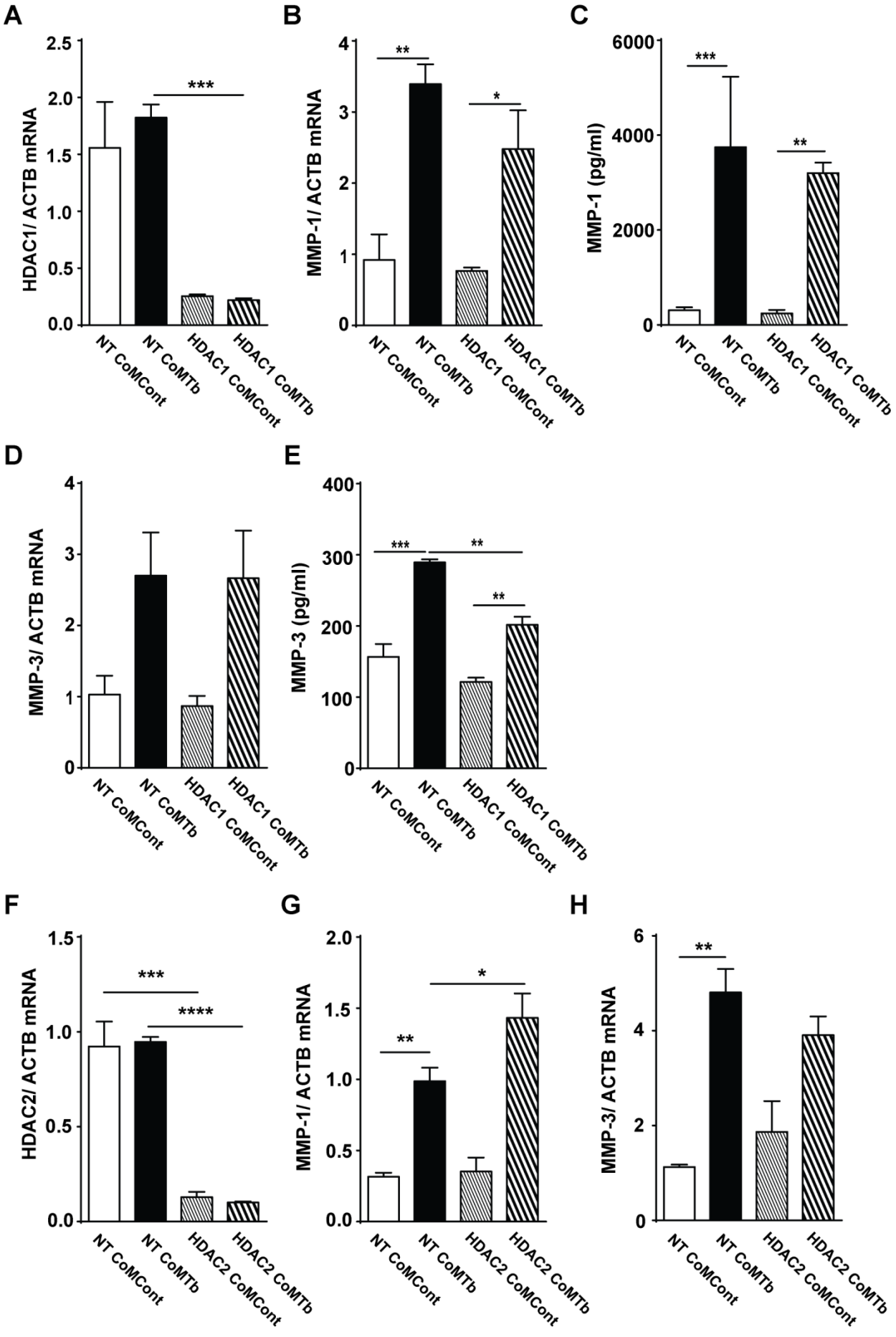
A
HDAC1/ ACTB mRNA
2.5
2.0
1.5
1.0
0.5
0.0
***
NT CoMCont
NT CoMTb
HDAC1 CoMCont
HDAC1 CoMTb
B
MMP-1/ ACTB mRNA
4
3
2
1
0
**
*
NT CoMCont
NT CoMTb
HDAC1 CoMCont
HDAC1 CoMTb
C
MMP-1 (pg/ml)
6000
4000
2000
0
***
**
NT CoMCont
NT CoMTb
HDAC1 CoMCont
HDAC1 CoMTb
D
MMP-3/ ACTB mRNA
4
3
2
1
0
NT CoMCont
NT CoMTb
HDAC1 CoMCont
HDAC1 CoMTb
E
MMP-3 (pg/ml)
400
300
200
100
0
***
**
**
NT CoMCont
NT CoMTb
HDAC1 CoMCont
HDAC1 CoMTb
F
HDAC2/ ACTB mRNA
1.5
1.0
0.5
0.0
***
****
NT CoMCont
NT CoMTb
HDAC2 CoMCont
HDAC2 CoMTb
G
MMP-1/ ACTB mRNA
2.0
1.5
1.0
0.5
0.0
**
*
NT CoMCont
NT CoMTb
HDAC2 CoMCont
HDAC2 CoMTb
H
MMP-3/ ACTB mRNA
6
4
2
0
**
NT CoMCont
NT CoMTb
HDAC2 CoMCont
HDAC2 CoMTb

Fig. 3

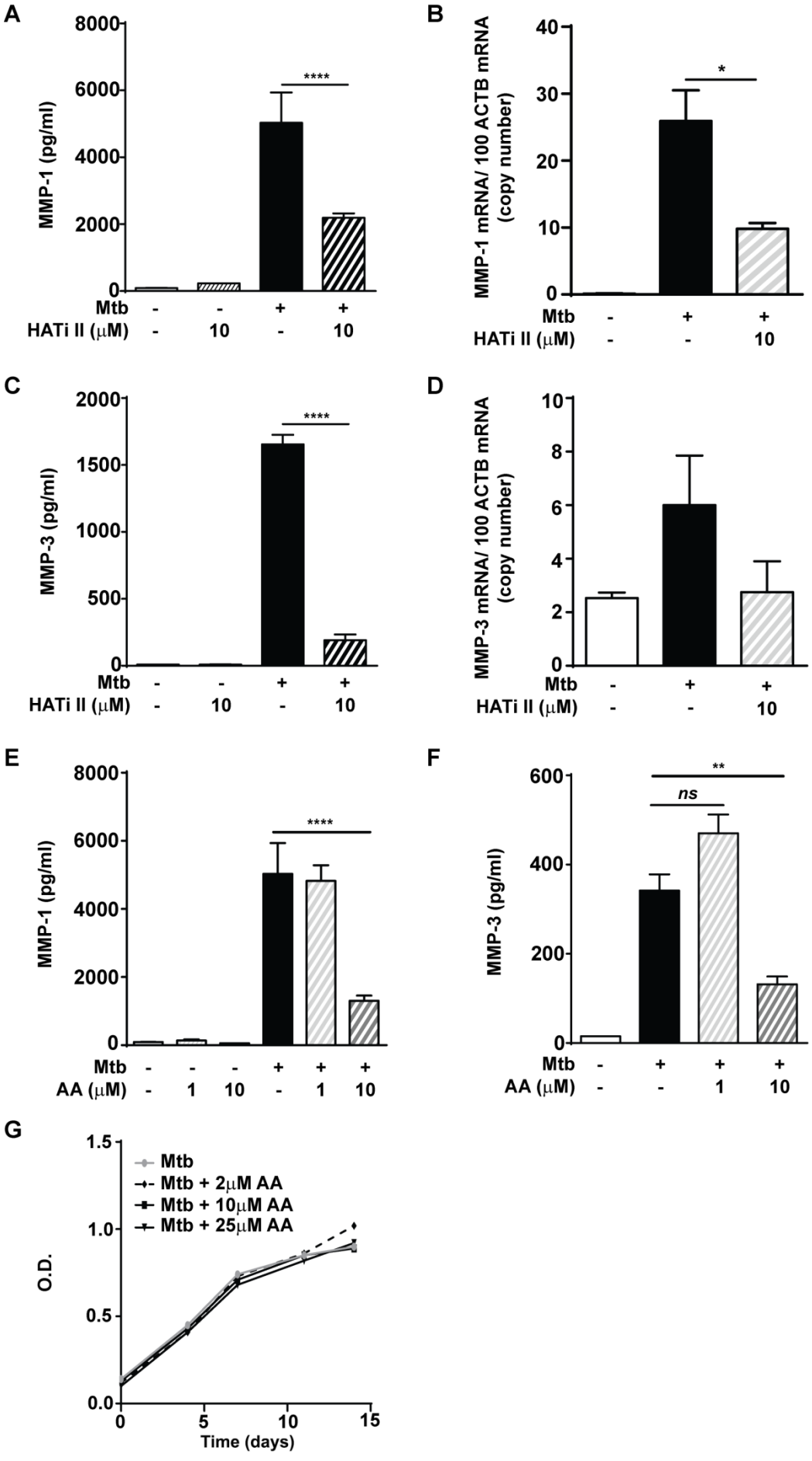
A
MMP-1 (pg/ml)
8000
6000
4000
2000
0
****
Mtb - - + +
HATi II (μM) - 10 - 10
B
MMP-1 mRNA/ 100 ACTB mRNA (copy number)
40
30
20
10
0
*
Mtb - + +
HATi II (μM) - - 10
C
MMP-3 (pg/ml)
2000
1500
1000
500
0
****
Mtb - - + +
HATi II (μM) - 10 - 10
D
MMP-3 mRNA/ 100 ACTB mRNA (copy number)
10
8
6
4
2
0
Mtb - + +
HATi II (μM) - - 10
E
MMP-1 (pg/ml)
8000
6000
4000
2000
0
****
Mtb - - - + + +
AA (μM) - 1 10 - 1 10
F
MMP-3 (pg/ml)
600
400
200
0
**
ns
Mtb - + + +
AA (μM) - - 1 10
G
O.D.
1.5
1.0
0.5
0.0
Mtb
Mtb + 2μM AA
Mtb + 10μM AA
Mtb + 25μM AA
0
5
10
15
Time (days)

Fig. 4

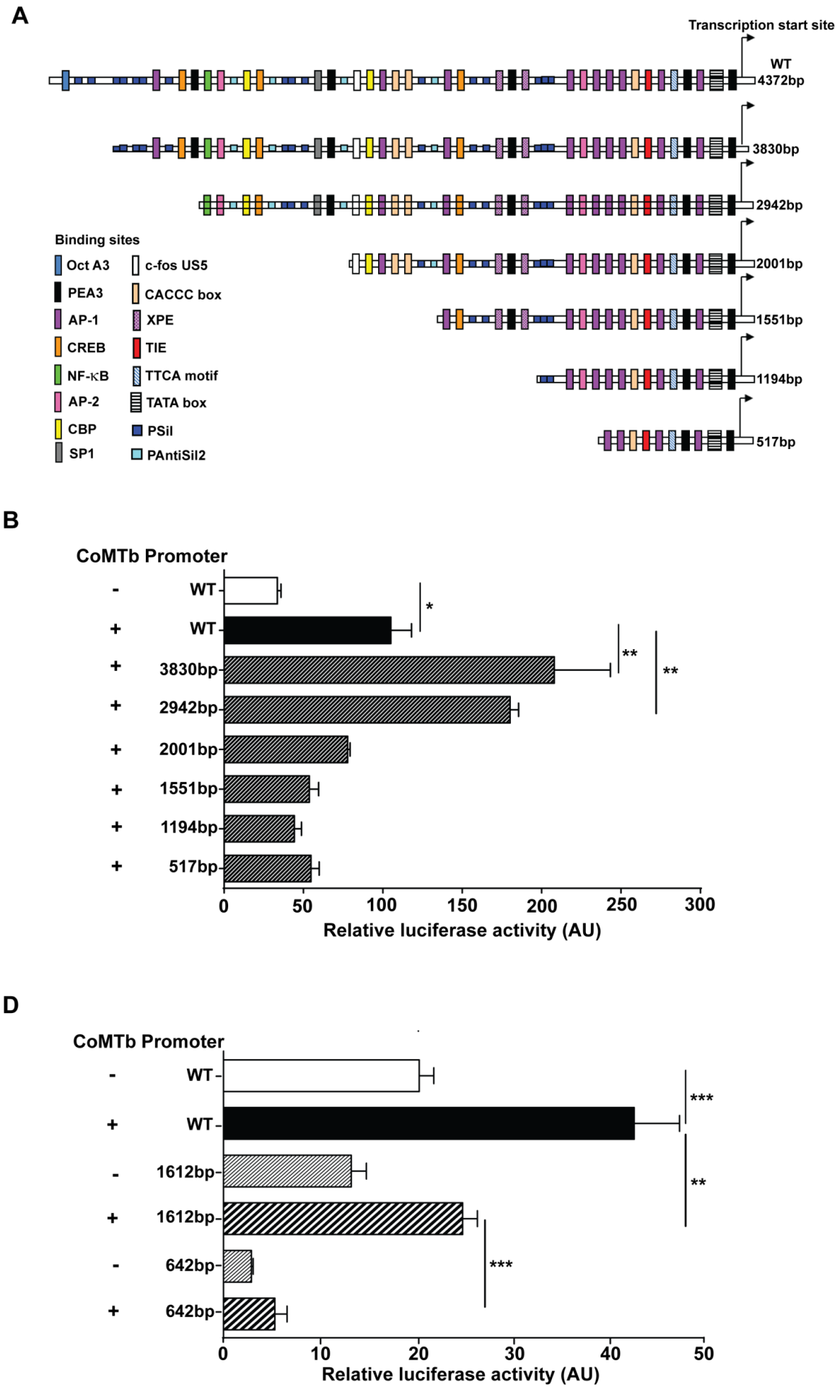
A
Transcription start site
WT
4372bp
3830bp
2942bp
2001bp
1551bp
1194bp
517bp
Binding sites
Oct A3
PEA3
AP-1
CREB
NF-κB
AP-2
CBP
SP1
c-fos US5
CACCC box
XPE
TIE
TTCA motif
TATA box
PSil
PAntiSil2
B
CoMTb Promoter
WT
WT
3830bp
2942bp
2001bp
1551bp
1194bp
517bp
Relative luciferase activity (AU)
D
CoMTb Promoter
WT
WT
1612bp
1612bp
642bp
642bp
Relative luciferase activity (AU)

Fig. 5

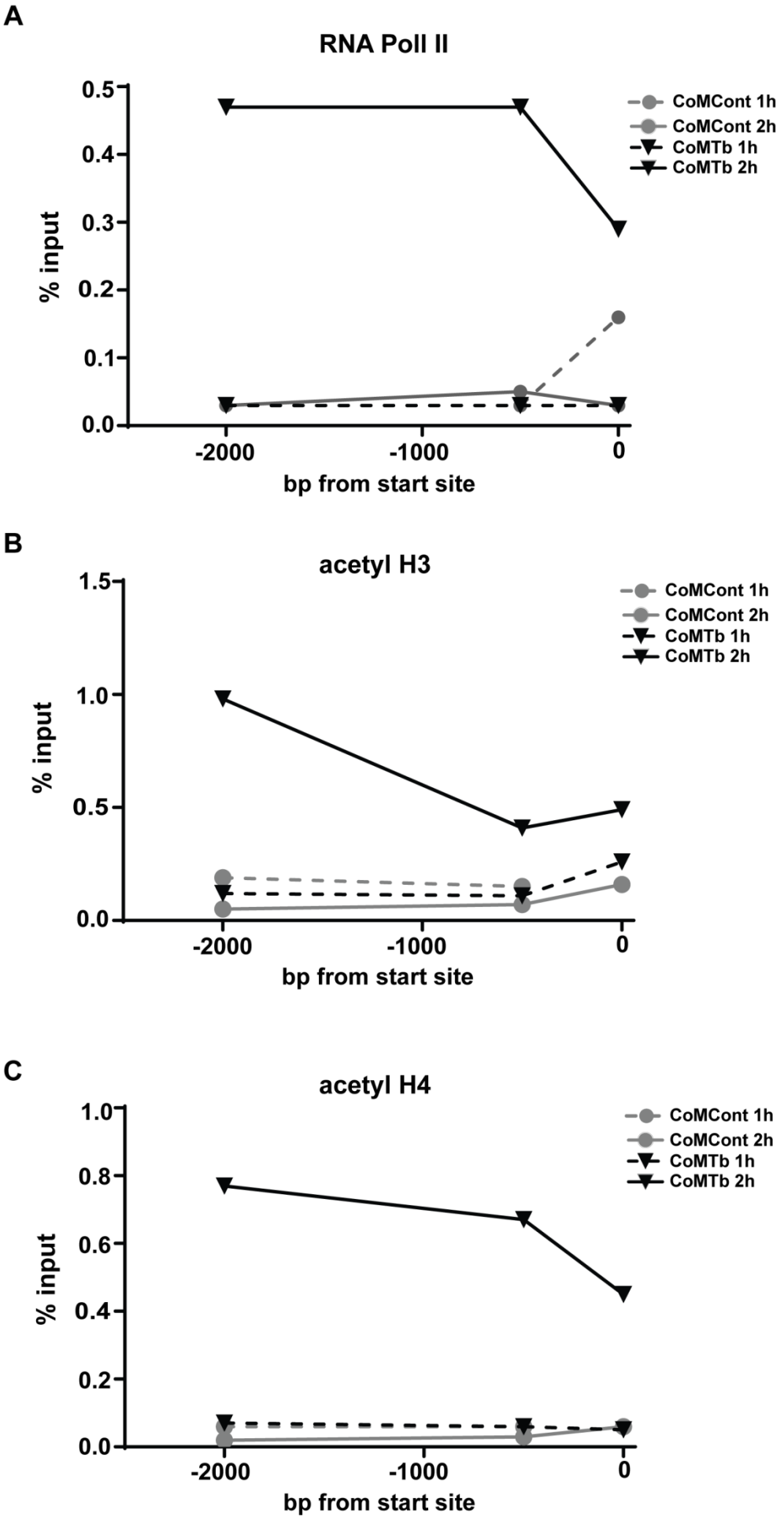
A
RNA Poll II
0.5
0.4
0.3
0.2
0.1
0.0
% input
-2000
-1000
0
bp from start site
CoMCont 1h
CoMCont 2h
CoMTb 1h
CoMTb 2h
B
acetyl H3
1.5
1.0
0.5
0.0
% input
-2000
-1000
0
bp from start site
CoMCont 1h
CoMCont 2h
CoMTb 1h
CoMTb 2h
C
acetyl H4
1.0
0.8
0.6
0.4
0.2
0.0
% input
-2000
-1000
0
bp from start site
CoMCont 1h
CoMCont 2h
CoMTb 1h
CoMTb 2h

Fig. 6

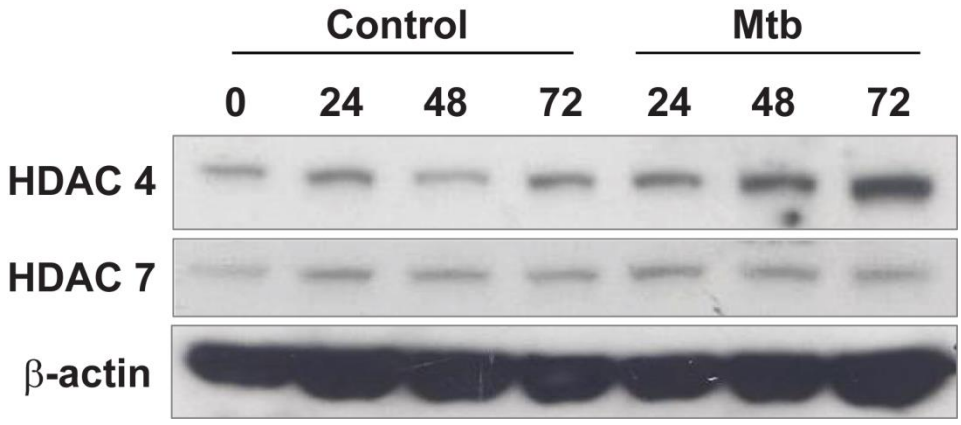

Figure S1- HDAC4 protein expression in Mtb-infected macrophages.

Macrophages were infected with H37Rv at MOI 1 for 24 to 72 hours and Western blots for HDACs 4 and 7 were performed on the cell lysates, and β-actin was used as loading control. HDAC 4 protein expression was more abundant in Mtb-infected cells at 48 and 72 hours post-infection, while HDAC7, a control HDAC which is stably expressed in macrophages, was unaffected.

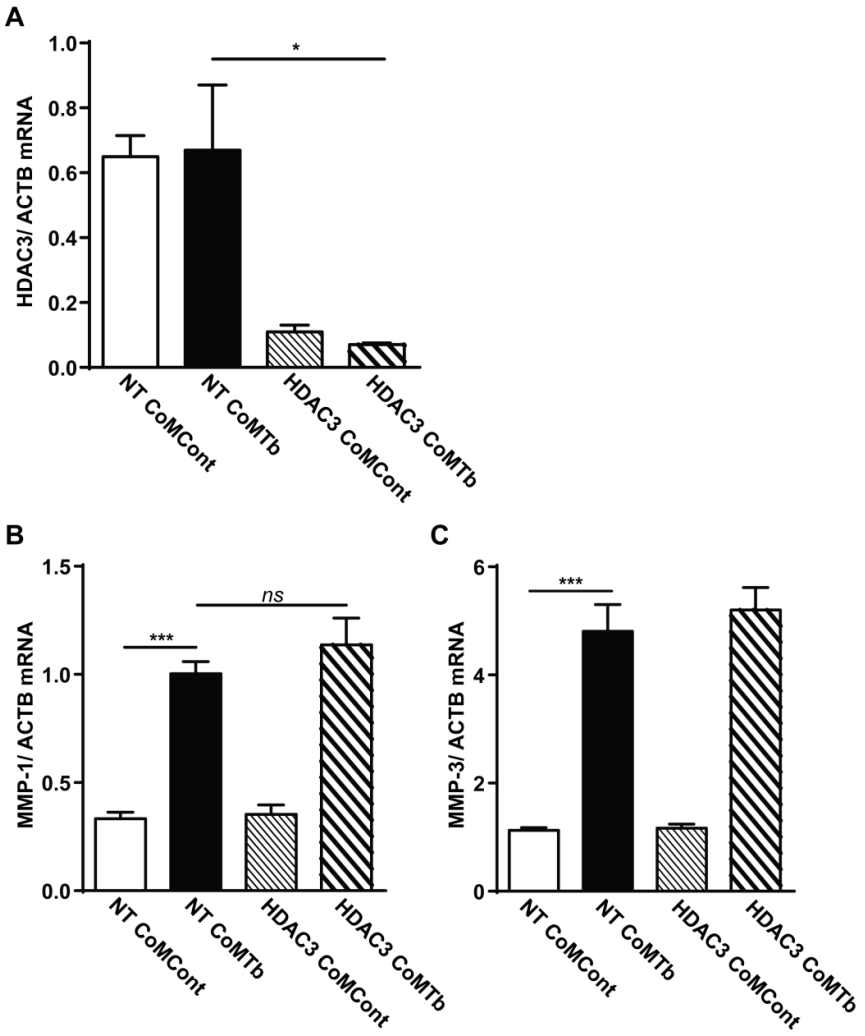

Figure S2- Silencing of HDAC3 expression does not inhibit CoMTb-driven MMP-1 and -3 gene expression.

NHBEs were transfected with 30nM non-targeting (NT) or HDAC3 specific siRNA. Cells were stimulated with CoMTb (1:5) for 24h. (A) HDAC3 mRNA normalized to the reference gene ACTB shows siRNA suppressed mRNA levels. (B) MMP-1 mRNA accumulation and (C) MMP-3 mRNA accumulation remained unchanged following HDAC3 silencing. mRNA of target genes was normalized to mRNA of the reference gene ACTB. Bars represent mean ± s.d. and analysis was performed using one-way ANOVA with Tukey's post-test.*$p<0.05$; ***$p<0.001$; ns- non significant. ACTB-beta-actin; HDAC3- histone deacetylase 3 siRNA; NT- non target siRNA.

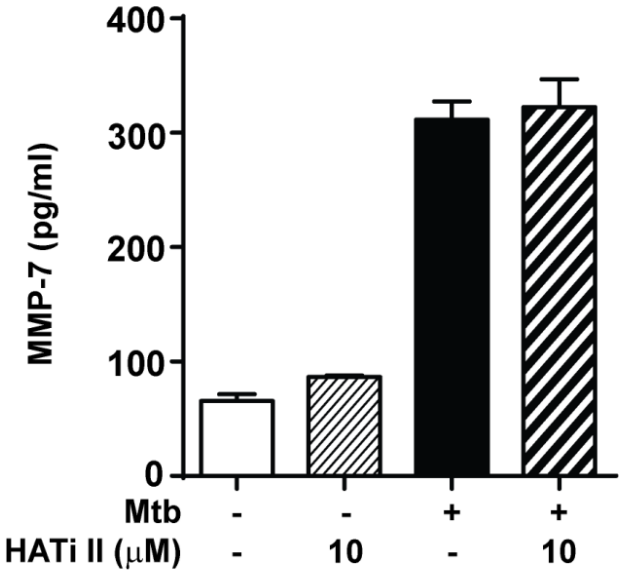

Figure S3- HATi II does not affect Mtb-driven MMP-7 secretion.

Macrophages were pre-incubated with 10μM HATi II prior to infection with H37Rv (MOI 1) and cell culture supernatants were collected after 72h. Pre-treatment with the HATi II did not affect MMP-7 secretion by Mtb-infected macrophages. Bars represent mean ± s.d. and analysis was performed using one-way ANOVA with Tukey's post-test.

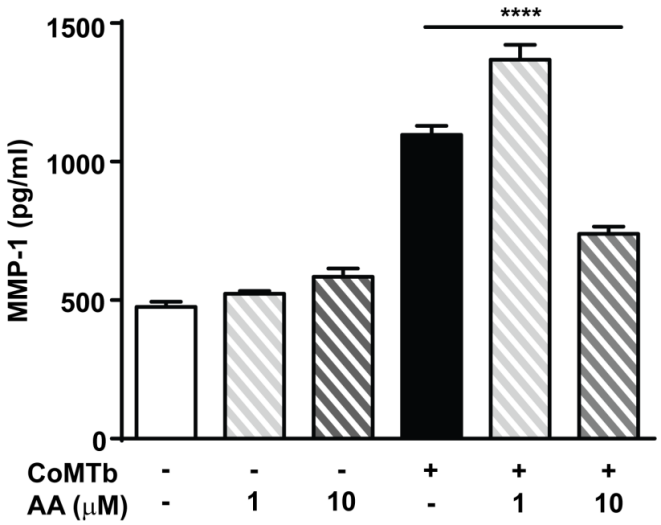

Figure S4- The HAT inhibitor Anacardic acid (AA) inhibits CoMTb-driven MMP-1 secretion in NHBEs.

NHBEs were pre-incubated with 1-10μM AA prior to CoMTb stimulation. Supernatants were collected after 72hrs and MMP-1 measured by ELISA. CoMTb-induced MMP-1 secretion is significantly inhibited by AA 10 μM. Bars represent mean ± s.d. and analysis was performed using one-way ANOVA with Tukey's post-test. ****$p<0.0001$; AA= anacardic acid.